Multiscale modelling of heat transfer from arrays of spherical particles

Conference Paper · May 2016

4 authors, including:

Schalk Cloete
SINTEF
48 PUBLICATIONS **227** CITATIONS
SEE PROFILE

Stefan Radl
Graz University of Technology
88 PUBLICATIONS **356** CITATIONS
SEE PROFILE

Shahriar Amini
SINTEF
45 PUBLICATIONS **248** CITATIONS
SEE PROFILE

Multiscale modelling of heat transfer from arrays of spherical particles

Arpit Singhal[1, 2], Schalk Cloete[3], Stefan Radl[4] and Shahriar Amini[3]*

[1] *NTNU (Norwegian University of Science and Technology)*
Department of Energy and Process Engineering
7051, Trondheim, Norway

[2] *University of Coimbra*
Department of Chemical Engineering
Rua Sílvio Lima, Pólo II
3030-790 Coimbra, Portugal
arpit.singhal@ntnu.no; arpit.singhal@sintef.no

[3*] *SINTEF Materials and Chemistry*
Flow Technology Department
S. P. Andersens veg 15 B,
Trondheim, Norway
Shahriar.Amini@sintef.no

[4] *Graz University of Technology*
Institute of Process and Particle Engineering
Inffeldgasse 13, 3rd floor,
8010 Graz, Austria

Abstract

This work presents a modelling study of gas-particle heat transfer on two distinct scales. Firstly direct numerical simulations (DNS) are conducted in a geometry of spherical particles generated via the discrete element method (DEM). Simulations are completed on random particle arrays ranging from a void fraction of 0.9 to maximum packing over a range of Reynolds numbers. The geometry is meshed with a fine Cartesian cut-cell mesh both inside and outside the particles. These DNS results are then used to provide improved heat transfer closures to an unresolved Lagrangian modelling approach which can be used to simulate much larger particle beds. This model is derived for two different averaging approaches and then verified against DNS data. Minor differences in results are discussed and heat transfer models derived from DNS with a constant heat source inside the particles are compared to models derived from simulations with a constant particle surface temperature.

Keywords: CFD-DEM, heat transfer correlation, packed bed, Eulerian-Lagrangian modelling, multiscale modelling

1. Introduction

Packed and fluidized bed reactors are broadly deployed in chemical, petrochemical and pharmaceutical industry. The prediction of transport parameters in such reactors is not an easy task and has been a central research topic for many decades.

Recently, DNS (Direct numerical simulation) for a coupled concept of CFD-DEM has emerged as a useful tool to obtain reliable predictions of heat transfer, considering the uncertainties involved in the experimental correlations. There are several correlations in the literature for heat transfer predictions utilising this concept of PR-DNS (particle resolved DNS).

An empirical correlation valid in both packed and fluidized beds over a range of porosity, Reynolds numbers and Prandtl numbers for heat and mass transfer was presented by Gunn [1]. The study by Tavassoli et al. [2] recently recommended the Gunn correlation [1] only for dilute systems with porosity (ε>0.7).

DNS is used to improve the accuracy of the model from Gunn [1] for monodisperse particles by increasing the range of porosity and Reynolds numbers [3, 4]. The concept of using PR-DNS to obtain a similar observation like Deen et al. [4] was introduced by Sun et al. [5, 6]. These models suggested an empirical correlation for packed beds with better prediction for heat and mass transfer.

Generally, a constant particle surface temperature is considered when modelling arrays of particles for deriving heat transfer correlations. This approach neglects the effects of intra particle temperature gradients which can lead to inhomogeneous particle surface temperatures. The only complete model to consider the conduction in packed beds is introduced by Oschmann et al. [7] hence representing the temperature distribution inside particles in a packed bed.

In this work, the goal is to develop correlations for heat transfer based on the non-homogenous temperature distribution via a constant heat source implemented in all particles. These results can then be compared with correlations derived from simulations with a fixed particle temperature. The comparison between the correlations to predict heat transfer with non-homogenous and homogenous particle surface temperatures is documented.

Then the verification of the correlation with homogenous surface temperatures is obtained by utilizing the correlation to predict the heat transfer in an unresolved Euler-Langrangian model implemented in CFDEM®-Coupling [8, 9]. Inclusion of the 1D model code PARSCALE [10] to account for the heat transfer inside the particles is a natural next step and will be a part of future work. Such an approach would pave the way for computationally efficient, yet accurate, predictions of fluid-particles systems characterized by large temperature gradients inside and outside of the particles.

*This work is a part of a European Union project under Seventh research framework programme (FP7/2007-2013) under grant agreement n° 604656 called NanoSim - A multi-scale Simulation based design platform for Cost effective CO2 capture Processes using Nano-structured materials. The authors are grateful to European Research Council for its support.

2. Methodology

2.1. DEM (particle bed generation)

In this work ANSYS FLUENT and Design Modeler are used to generate the packed bed using the DEM (Discrete Element Method) approach according to Table 1. The particles are injected in the reactor geometry without the gravity force with a high degree of overlap. Large repulsive forces are generated because of these overlapping particles, thus initiating random particle motions. After 20 s of random translation and collision of the particles in the DEM simulation, the resulting random packed bed of the particles is obtained. Particle positions are exported to Design Modeler and particles which are very close to each other are cut with a small cylindrical geometry to ensure at least $d_p/25$ m of space between all particles. This results in a geometry which can be meshed with a good quality mesh.

Table 1: DEM simulation setup.

Parameters	Law	Value
Number of particles		350
Diameter of the particles (d_p) (m)		0.001
Particle normal force Spring Dashpot for DEM	Spring dashpot	*K* = 1250 *Eta* = 0.9
Particle tangential force parameter for DEM	Friction-dshf	*mu-stick* = 0.5 *mu-glide* = 0.2 *mu-limit* = 0.1
Time step (s)		$5x10^{-05}$

2.2. Mesh

The packed bed reactor geometry is meshed with the cutcell method using ANSYS Meshing both inside and outside the particles. Table 2 shows the details of the mesh parameters.

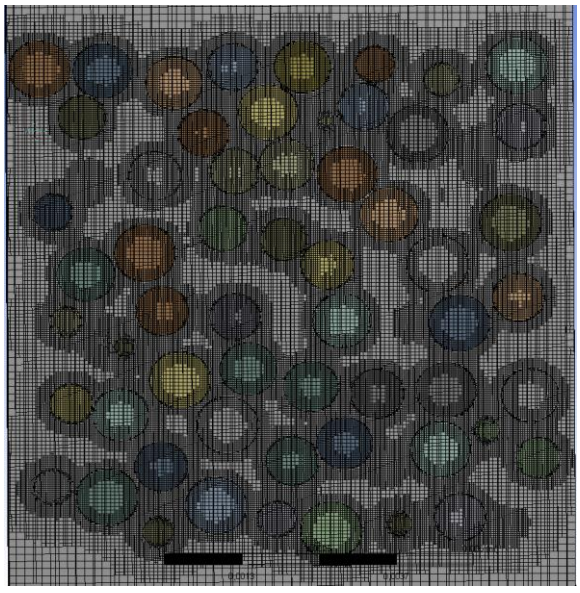

Figure 1: The section (y=0) of the reactor geometry with cutcell mesh.

Table 2: Mesh sizing details.

Parameters	Value
The cell size of surface mesh on the particles (m)	$4e^{-05}$
Maximum face size for the mesh (m)	$2e^{-04}$
Resolution of mesh on particles for DNS	$d_p/25$
Growth rate of mesh	1.2

2.3. CFD

ANSYS FLUENT is used to perform the DNS in the resulting geometry. The SIMPLE algorithm with 2nd order spatial discretization is used for the DNS simulations. Further details of the simulation are given below.

2.3.1 Model equations

The conservation equations of continuity, momentum, and energy for the incompressible, steady state, Newtonian fluid solved for the DNS in this paper are given by

$$\nabla.\vec{u} = 0 \tag{1}$$

$$\nabla.(\rho\vec{u}\vec{u}) = -\nabla p - \mu\nabla^2\vec{u} + \rho\vec{g} \tag{2}$$

$$\rho C_p \nabla.(T\vec{u}) = K_f \nabla^2 T \tag{3}$$

Steady DNS was found to be sufficient as transient fluctuations were not forming in the channels between particles at the Reynolds numbers investigated in this work.

The particle equation of motion for the DEM simulations is given by:

$$m_P \frac{dv}{dt} = m_P g + \sum_{i=1}^{j} (F_{P,i,n} + F_{P,i,t}) \tag{4}$$

Rotational particle motion was not solved as this was not necessary to obtain a randomly dispersed particle array.

2.3.2 Boundary conditions

A velocity inlet was specified at the bottom of the geometry and pressure outlet at the top. No-slip walls were specified with zero heat flux. The particles either contained a constant heat source of 10^7 W/m^3 or a constant temperature of 573 K. Table 3 shows all the flow properties used for the CFD simulations.

Table 3: Parametric flow properties.

Parameter	Value
Density (ρ) (kg/m^3)	1
Viscosity (μ) (kg/m s)	10^{-05}
Thermal conductivity (k) (W/m K)	0.01
Specific Heat capacity (C_p) (J/kg K)	1000
Prandtl number	1
Temperature at the Inlet (K)	473
Volumetric heat source integrated in particles for heat source correlation (W/m^3)	10^7
Constant Temperature on particles for constant temperature correlation (K)	573

$$\varphi_{P\to f} = h\,(T_{P,av} - T_{bulk}); \text{ or} \quad (5)$$
$$\varphi_{P\to f} = h\,(T_{P,av} - T_{av})$$

The heat transfer coefficient *(h)* is computed from the particle surface heat flux $(\varphi_{P\to f})$ using Eqn. (5), where (T_P) is the average for all the particle surface temperatures, (T_{bulk}) is the bulk fluid temperature and (T_{av}) is the average fluid temperature. Two different averaging procedures for T_{bulk} and T_{av} are discussed in Section 2.4.

2.4. Averaging procedure

The exact procedure for computing the locally-averaged fluid temperature experienced by the particles in the reactor is relevant, since it directly impacts the local heat transfer coefficient. Therefore, the concept of the bulk fluid temperature (T_{bulk}) used by Deen et al. [3] can be followed, suggesting that the fluid temperature should be computed in several planes perpendicular to the flow direction. Deen et al.'s approach is based on the so-called cup-mixing temperature, i.e., a flux-weighted temperature. In contrast, Sun et al. [5] used the average fluid temperature (T_{av}) to obtain the heat transfer predictions. In this paper both approaches are evaluated, and bulk as well as the average fluid temperatures are calculated. These temperatures are then used to formulate correlations, which are then verified against the unresolved model to obtain the correct averaging procedure.

The averaging procedures are given in Eqn. (6) and Eqn. (7) showing the bulk fluid temperature and average temperatures respectively; where T is the static fluid temperature:

$$T_{bulk} = \frac{\int (u.e_z) T\, dV}{\int (u.e_z)\, dV} \quad (6)$$

$$T_{av} = \frac{\int T\, dV}{\int dV} \quad (7)$$

2.5 Non resolved Eulerian-Lagrangian simulations

The non-resolved simulations involve the usage of the DEM open source package LIGGGHTS [9] for generation of the packed bed and CFDEM-Coupling [8] for the CFD simulations. The CFD and DEM code generally perform their calculations separately in parallel and exchange data in accordance with the coupling intervals specified.

In non-resolved Eulerian-Lagrangian simulations the particles are not resolved, which means that particle sizes should be smaller than the computational grid (Figure 2), making this simulation much less computationally costly than the resolved simulations. The interaction of the particle phase with the fluid phase in terms of the momentum, energy and mass transfer is considered. This is facilitated by using the appropriate correlations to account for the transfer. The correlations obtained in this work are applied to model heat transfer, while momentum transfer is modelled via the KochiHill drag model.

3. Results and discussions

A consistent correlation to predict the heat transfer in the packed bed is obtained using three different randomly packed beds over a range of porosity values and Reynolds numbers. The effect of change in the Prandtl number is not considered currently as the Prandtl number does not vary a great deal for gaseous flows. The details of the different cases simulated to obtain the correlation are given in Table 4.

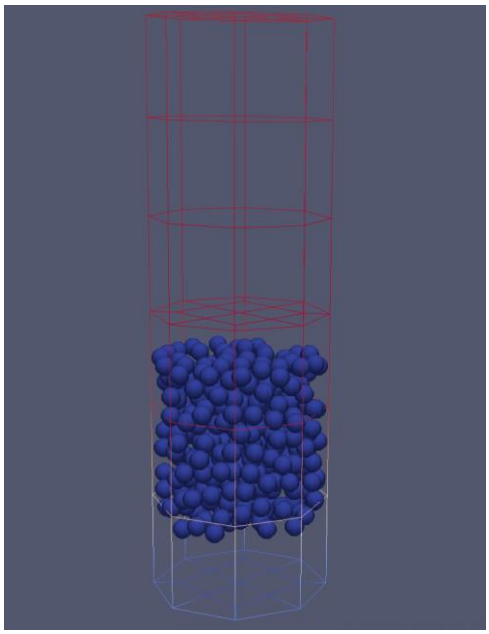

Figure 2: Non-resolved Eulerian-Lagrangian grid setup

Table 4: Representation of the cases simulated

Parameters	Value
Number of particles in the reactor	350
Particle diameter size (m)	10^{-3}
Bed Porosities (ε)	0.42; 0.62; 0.87
Reynolds numbers simulated	10; 40; 70; 100

3.1. Heat transfer in randomly arranged packed beds

The results for the heat transfer coefficient from spherical particles (with a non-homogenous particle surface temperature) in the packed bed is simulated for different Reynolds numbers and bed porosities as shown in Table 4. This data is then benchmarked against the correlations of Gunn et al., Deen et al. and Sun et al. [1, 4, 5]. Figure 3 shows the temperature variations with the change in Reynolds numbers and the bed porosity. Temperature gradients inside the particle are observed, which depend on the Reynolds number.The plots for the convective heat transfer inside the region of interest (which is located far from the wall, as well as the inlet and the outlet to avoid effects due to an inhomogeneous bed structure) are shown in Figure 4. It is seen that the results agree with the correlations in case the bulk fluid temperature (T_{bulk}) is considered when computing the heat transfer coefficient. In contrast, the heat transfer coefficient that relies on the average fluid temperature (T_{av}) significantly differs from literature correlations. We can only speculate what is the origin of this difference, which has been also observed by Sun et al. [5]. Certainly, one argument is that existing correlations are limited by the assumption of a fixed particle surface temperature, which is not the case in simulations using a fixed volumetric heat source. Clearly, a more detailed analysis of the variation of the particle surface temperature is needed in order to probe the exact origin for the observed differences.

3.2. Heat transfer correlation

Nusselt number correlations for the fluid-particle heat transfer in the random particle array with non-homogenous particle surface temperature and homogenous particle surface temperature are obtained by fitting the data obtained over different porosities and Reynold numbers.

The effect of the change in Prandtl is not considered in this current correlation (i.e., we assume $Pr = 1$). The correlation is valid over a porosity range ($0.4 < \varepsilon < 0.9$) and particle Reynolds number (Re_p<100).

The correlation is fitted in the structure of the Gunn correlation. Two different methods to compute the fluid temperature described in Section 2.4 are used to obtain different correlations according to the method of computing fluid temperature.

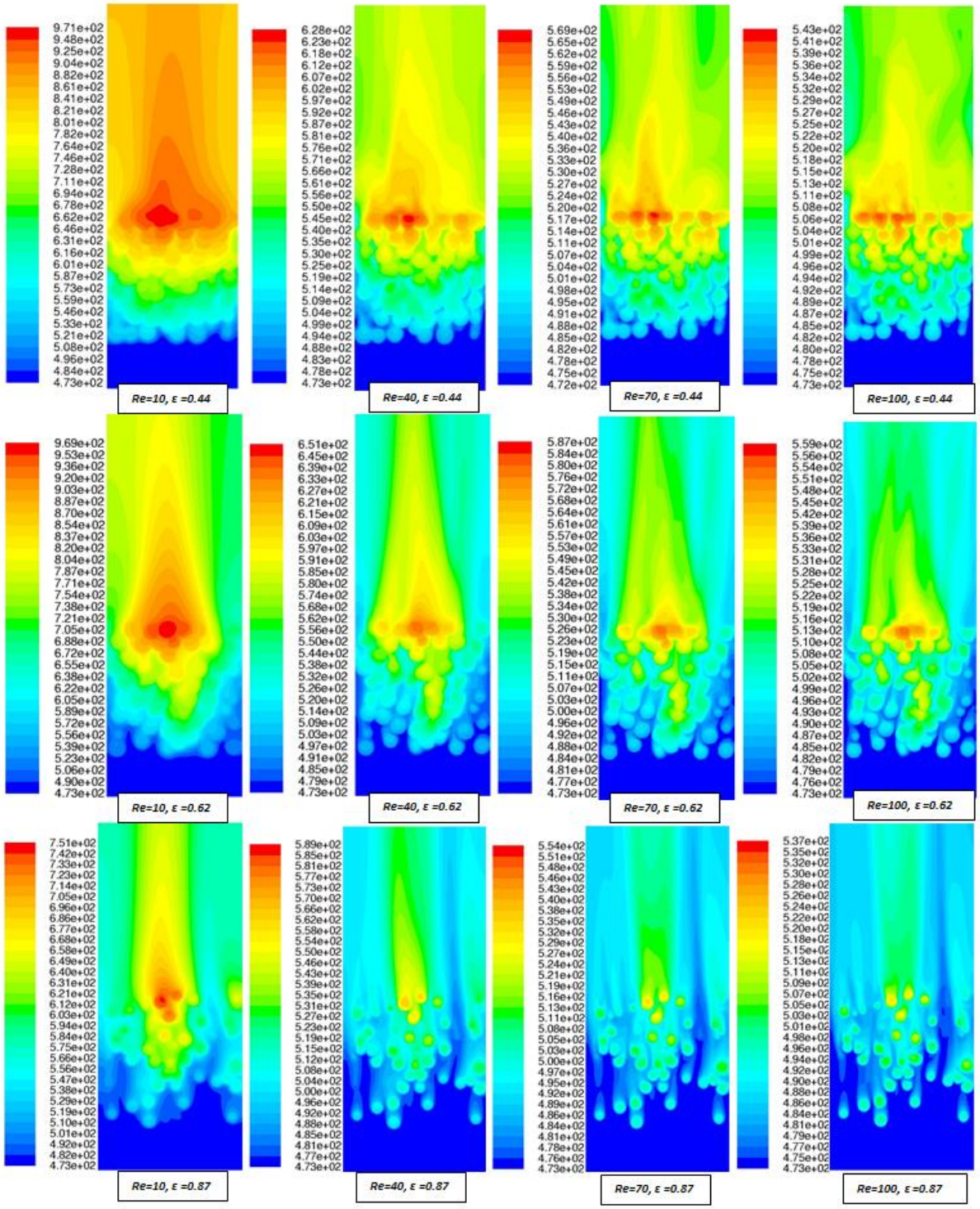

Figure 3: Temperature distribution profiles with temperature gradients inside the particles at plane y=0, through the reactor geometries with different bed porosities and Reynolds numbers for the case with a fixed volumetric heat source inside the particles.

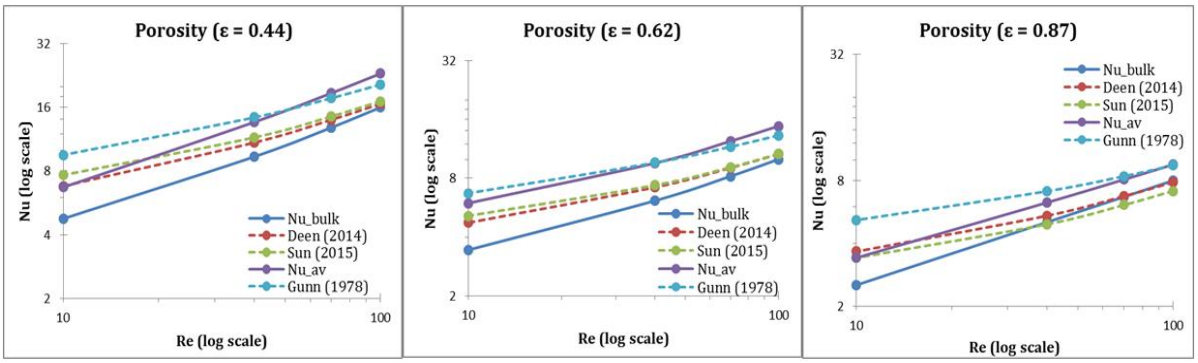

Figure 4: Comparison of the heat transfer coefficient in the region of interest (no wall, inlet and outlet effects) over different porosity and Reynolds number values for the case with integrated heat source inside the particles.

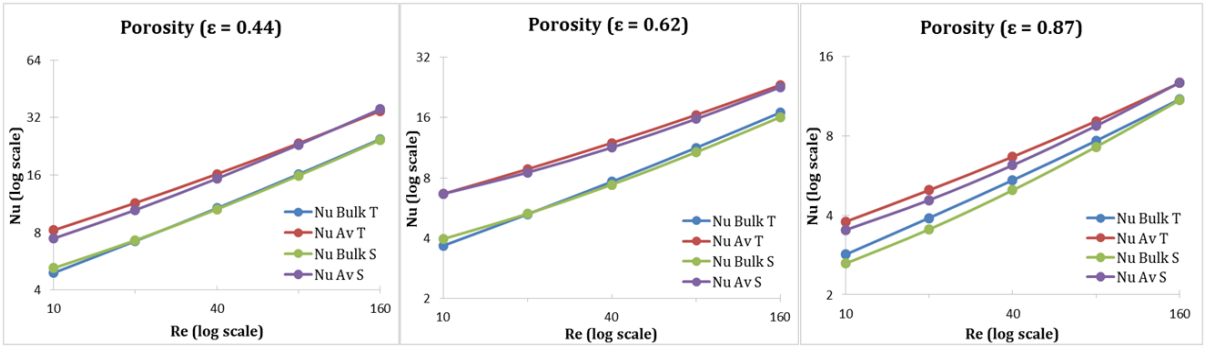

Figure 5: Comparison of the prediction of heat transfer from the correlations obtained in this work. T = constant temperature (homogenous particle surface temperature); and S = integrated heat source (non-homogenous particle surface temperature.

The correlations for non-homogeneous particle surface temperature are as follows for volume averaged (Eqn (7)) and bulk (Eqn (6)) fluid temperatures:

$$Nu_{bulk} = (0.455 + 5.09\varepsilon - 5.05\varepsilon^2)(0.67 + 0.35Re^{0.2}) + (1.73 - 3.38\varepsilon + 1.95\varepsilon^2)(Re^{0.7}) \quad (6)$$

$$Nu_{av} = (-1.42 + 6.43\varepsilon - 5.12\varepsilon^2)(3.2 + 2.54Re^{0.2}) + (2.9 - 6.13\varepsilon + 3.59\varepsilon^2)(Re^{0.7}) \quad (7)$$

The same correlations are given for the case with constant particle surface temperature in Eqns (8) and (9).

$$Nu_{bulk} = (2.844 - 3.49\varepsilon + 2.36\varepsilon^2)(-0.71 + 1.17Re^{0.2}) + (1.4 - 2.35\varepsilon + 1.12\varepsilon^2)(Re^{0.7}) \quad (8)$$

$$Nu_{av} = (-0.3 + 6.87\varepsilon - 6.31\varepsilon^2)(-1.08 + 2.60Re^{0.2}) + (2.28 - 4.58\varepsilon + 2.51\varepsilon^2)(Re^{0.7}) \quad (9)$$

3.3 Comparison of the correlations with non-homogenous vs homogenous particle temperature

Figure 5 compares the four different correlations described in Section 0 over a range of Reynolds numbers. It is immediately clear that a large different between the correlations using bulk and average temperatures exists. The difference in the correlations using uniform and non-uniform particle surface temperatures is smaller, but does become significant for the highest porosity considered. It is reasoned that higher porosities create sufficient space between particles to allow a wake region to be established behind the majority of particles. As a result, the convective heat transfer behind the particle is slower than at the front, leading to an asymmetric temperature profile in the particle with higher surface temperatures behind the particle. The hottest part of the particle surface is therefore exposed to the slowest moving fluid and vice versa, thus creating a heat transfer limitation which requires a higher average particle surface temperature to attain a given surface heat flux.

3.4 Comparison between the resolved and unresolved models

The correlations obtained with a homogenous particle surface temperature are used to account for the heat transfer in the non-resolved Euler-Lagrangian simulations. The particle bed with a porosity of 0.62 is replicated in LIGGGHTS® and the CFDEM® simulation, with identical flow properties as in the PR-DNS using FLUENT.

Figure 6 shows that fluid temperature is better approximated when using the correlation for the Nusselt number obtained from bulk fluid temperature. Therefore, it appears that the bulk fluid temperature is a better option for predicting heat transfer in the packed beds. However, predictions of the CFD-DEM simulation differ from the PR-DNS results in a significant for both correlations. We speculate that one possible reason for this is that in CFD-DEM-based simulations the local porosity of the bed is only insufficiently approximated. Clearly, a more in-depth analysis of the local porosity and Reynolds number experienced by particles in case of CFD-DEM-based simulations is needed to probe the origin of the observed differences.

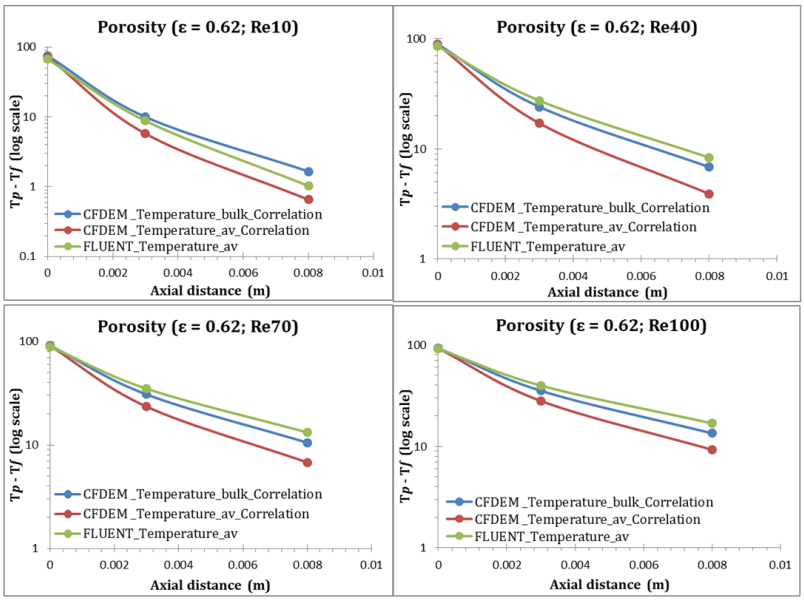

Figure 6: Comparison of the predicted fluid temperature between CFDEM results and FLUENT results on cross-stream planes in the bed. T_p = Particle surface temperature and T_f = Area weighted fluid temperature in the plane

4. Summary and conclusions

This work presented two different approaches for predicting heat transfer in narrow packed bed reactors that are confined by cylindrical walls. First, using resolved DNS, heat transfer rates are directly computed for both (i) a fixed particle surface temperature, and (ii) a fixed volumetric heat source inside the particles. This exercise allowed us to establish in total four heat transfer correlations. Second, non-resolved simulations are performed, which are computationally cheaper, and hence more efficient. Heat transfer rates are predicted using the developed correlations, and differences are analysed.

Specifically, whether to use the bulk fluid temperature or the average fluid temperature to predict the transferred amount of heat in packed beds is probed. It is observed that the correlation relying on the bulk fluid temperature yields predictions (when using unresolved Euler-Lagrangian simulations) that are in better agreement with results from PR-DNS. However, still significant differences between unresolved and PR-DNS are visible. The origin of these deviations could not be probed in the present work. However, we speculate that these are possibly connected to (i) wall effects, and (ii) the details of the void fraction reconstruction in case of unresolved Euler-Lagrangian simulations.

5. Acknowledgements

The authors would like to express their gratitude for the financial support from the European Commission under the NanoSim grant (project number: 604656).

References

[1] Gunn, D.J., *Transfer of heat or mass to particles in fixed and fluidised beds.* International Journal of Heat and Mass Transfer, 1978. **21**(4): p. 467-476.

[2] Tavassoli, H., E.A.J.F. Peters, and J.A.M. Kuipers, *Direct numerical simulation of fluid–particle heat transfer in fixed random arrays of non-spherical particles.* Chemical Engineering Science, 2015. **129**: p. 42-48.

[3] Deen, N.G., et al., *Direct numerical simulation of flow and heat transfer in dense fluid–particle systems.* Chemical Engineering Science, 2012. **81**: p. 329-344.

[4] Deen, N.G., et al., *Review of direct numerical simulation of fluid–particle mass, momentum and heat transfer in dense gas–solid flows.* Chemical Engineering Science, 2014. **116**: p. 710-724.

[5] Sun, B., S. Tenneti, and S. Subramaniam, *Modeling average gas–solid heat transfer using particle-resolved direct numerical simulation.* International Journal of Heat and Mass Transfer, 2015. **86**: p. 898-913.

[6] Tenneti, S., et al., *Role of fluid heating in dense gas–solid flow as revealed by particle-resolved direct numerical simulation.* International Journal of Heat and Mass Transfer, 2013. **58**(1–2): p. 471-479.

[7] Oschmann, T., M. Schiemann, and H. Kruggel-Emden, *Development and verification of a resolved 3D inner particle heat transfer model for the Discrete Element Method (DEM).* Powder Technology, 2016. **291**: p. 392-407.

[8] Goniva, C., et al., *Influence of rolling friction on single spout fluidized bed simulation.* Particuology, 2012. **10**(5): p. 582-591.

[9] Kloss, C., et al., *Models, algorithms and validation for opensource DEM and CFD–DEM.* Progress in Computational Fluid Dynamics, an International Journal, 2012. **12**(2-3): p. 140-152.

[10] S. Radl, T.F., A. Aigner, and C. Kloss. *An Open-Source Library for the Simulation of Intra-Particle Heat and Mass Transport Processes in Coupled Simulations.* in *IV International Conference on Particle-based Methods Fundamentals and Applications (PARTICLES 2015),*. 2015. Barcelona, Spain.